RSC Advances

PAPER

View Article Online
View Journal | View Issue

Cite this: *RSC Adv.*, 2019, **9**, 40845

Facile synthesis of laccase mimic Cu/H_3BTC MOF for efficient dye degradation and detection of phenolic pollutants†

Saira Shams, Waqas Ahmad, Amjad Hussain Memon, Yun Wei, Qipeng Yuan* and Hao Liang*

Herein, we report an effectual method for designing a novel form of nanozyme laccase mimic namely Cu/H_3BTC, using copper ions and 1,3,5-benzene tricarboxylic acid (1,3,5-H_3BTC). This Cu-based metal–organic framework (MOF) was synthesized through a simple procedure of mixing of two usual reagents at room temperature. Amido Black 10B (AB-10B) was chosen as a model dye for degradation consequences. Results showed that Cu/H_3BTC MOF revealed significantly higher catalytic efficacy under certain conditions like high pH, extreme temperature and high salt conditions and it has long-term storage stability, which can lead to a significant decline in catalytic activity of laccase. In addition, the degradation of AB-10B was up to 60% after ten cycles, showing good recyclability of Cu/H_3BTC MOF. The UV-visible spectral changes clearly showed that Cu/H_3BTC MOF is an effective laccase mimic for the degradation of azo dye AB-10B, which was degraded more easily within the time duration of 60 min. The Cu/H_3BTC MOF also possessed fundamental activities like laccase with regard to oxidation of the phenolic compounds. Moreover, a technique for the quantitative detection of epinephrine by Cu/H_3BTC MOF was established. These findings help to understand the laccase-like reactivity and provide a basis for the future design and application of metal-based catalysts.

Received 17th September 2019
Accepted 2nd December 2019

DOI: 10.1039/c9ra07473b

rsc.li/rsc-advances

1. Introduction

Azo dyes associated with various industries as synthetic colorants have caused environmental contamination as a consequence of their release in waste streams during operating procedures.[1] Mostly azo dyes are recognized to be non-biodegradable in aerobic conditions while in anaerobic conditions they are reduced to most dangerous intermediate products.[2] Furthermore, most of the dyes are considered to be poisonous and carcinogenic, therefore their removal from waste water is one of the crucial concerns.[3–5] Several chemical–physical techniques of dye degradation or decolorization have been employed but they are generally outdated because of some unsolved issues.[6–8]

Natural enzymes could effectively degrade toxic wastes but they are very delicate in nature due to their limited applications in harsh conditions.[9–11] Recently, nanozymes, a kind of artificial nano catalyst with similar characteristics to natural enzymes are getting enormous interest.[12] The nanozymes possessed better stability, notable catalytic activity and low cost as compared to natural enzymes.[13–15] Therefore, the synthesis of nanozymes emerges as a source in nano-science to replace natural enzyme.

Laccases are multicopper oxidases which has an important role in dye degradation[16] as well as catalyse oxidation reactions of various substrates.[17,18] Due to unstable nature and low yield of laccase, different approaches have been reported to develop laccase-like materials.[19–26] But their laccase activity was not good enough compare to natural enzymes and still highly desirable to be studied due to wide range of applications.

Metal–organic frameworks (MOFs) have been reported before with enormous results in different applications.[27–31] The removal of risky and harmful substances like dyes and sulphur comprising constituents has also been analysed using MOFs.[32–34] However, for the time being there has been limited reports on MOFs for the removal of dye materials. Furthermore, investigations on MOFs for dye removal are yet unsatisfactory. Hence, it is an important task to obtain MOF which would exhibit great ability towards dye degradation.

In the previous studies different ligands have been used to construct and design functional materials and mimicking biological systems.[35–42] The ligand H_3BTC has not been studied more to show the mimic enzyme nature whereas Cu ions are well known to show the enzyme mimic nature. Therefore, we hypothesized that coordination of Cu with H_3BTC could expose excellent laccase like enzyme mimic nature. However, no one

State Key Laboratory of Chemical Resource Engineering, Beijing University of Chemical Technology, Beisanhuan Donglu 15 Hao, Beijing 100029, P. R. China. E-mail: lianghao@mail.buct.edu.cn; yuanqp@mail.buct.edu.cn; Fax: +86 10 64437610; Tel: +86 10 64431557

† Electronic supplementary information (ESI) available. See DOI: 10.1039/c9ra07473b

has reported before to use H_3BTC ligand to show laccase like mimic activity.

Herein, we developed an innovative and convenient strategy for synthesizing Cu/H_3BTC MOF as an alternative of laccase, presenting a first step toward their use with activity similar to laccase. Thus, the objective of present study was to evaluate the efficiency of Cu/H_3BTC MOF against dye degradation, various parameters that influence degradation of dye and to investigate the laccase like behaviours towards phenolic compounds. Cu/H_3BTC MOF showed prominent enzyme mimic activity comparative to natural laccase. Amido Black 10B (AB-10B) dye was chosen for degradation by Cu/H_3BTC MOF and was reported with excellent results than natural enzyme with profound stability and reusability. Furthermore, the UV/vis spectral changes of AB-10B by Cu/H_3BTC MOF was also studied. This demonstrates that Cu/H_3BTC MOF have great potential in enzyme catalysis and degradation.

2. Experimental

2.1. Materials

H_3BTC (1,3,5-benzene tricarboxylic acid) and 2,4-DP (2,4-dichlorophenol) was obtained from J&K Chemical Ltd. (Beijing, China). GMP (guanosine 5′-monophosphate disodium salt hydrate), AMP (adenosine 5′-monophosphate disodium salt), CMP (cytidine 5′-monophosphate disodium salt), 4-AP (4-aminoantipyrine), MES monohydrate (2-(morpholino)ethanesulfonic acid), AB-10B (Amido Black 10B) dye and all the metal salts were procured from Aladdin Inc, (Shanghai, China). Laccase was purchased from Yuanye Biotechnology Co., Ltd. (Shanghai, China). HEPES (4-(2-hydroxyethyl)-1-piperazine ethane sulfonic acid) was from Tianjin Heowns Biochem. Llc. (Shanghai, China). Milli-Q water was used for the preparation of solutions and buffers. All the solvents and chemicals were of analytical grade and used as achieved.

2.2. Preparation of Cu/H_3BTC MOF

The Cu/H_3BTC MOF was prepared by adding 200 μL of H_3BTC (25 mM), 700 μL HEPES buffer (pH 8.0, 10 mM) and 100 μL $CuCl_2$ (50 mM). After that samples were incubated at room temperature. One hour later, centrifuged the samples (10 000 rpm, 5 min) to remove the supernatants and the obtained precipitates were mixed with 1 mL de-ionized water for volume balance. Freshly prepared samples were used for the further experimental steps.

2.3. Characterization of Cu/H_3BTC MOF

The as synthesized MOF was freeze-dried to get solid fine particles and was characterized by XRD (X-ray diffraction), FTIR (Fourier transform infrared spectroscopy), SEM (scanning electron microscopy) and XPS (X-ray photoelectron spectroscopy). XRD was conducted on an X-ray diffractometer (Bruker, Germany). FTIR was performed on FTIR spectrometer (Nicolet, Waltham, MA, USA). SEM was carried out on a Hitachi S-4700 microscope fitted with a Phoenix energy dispersive X-ray analyser (EDS S2 Ranger, Bruker, Germany). N_2 adsorption/desorption isotherms was achieved with a Surface Area Analyzer (V-SORB 4800S). XPS was performed on XPS spectrometer (Kratos Axis Supra). Zeta potential was recorded using Zeta sizer Nano-ZS (Malvern, England). UV-visible spectrophotometer (U3010, Hitachi, Tokyo, Japan) was employed for overall enzymatic studies. The catalytic activity was estimated *via* disclosure to UV radiation for a duration of 60 min.

2.4. Effect of Cu/H_3BTC MOF and laccase on AB-10B degradation

To analyse the degradation influence of AB-10B dye with passage of time by Cu/H_3BTC MOF and laccase, experiment was carried out over the range of 60 min. UV-visible spectrophotometer was used to measure the concentration change of AB-10B dye at different time interval in the range of 200–700 nm. Prior to processing, maximum absorbance wavelength of AB-10B dye at 620 nm might be regarded from the spectrum. Hence, at different reaction times residual dye concentration was determined by measuring the absorption intensity at 620 nm. For degradation experiment, 300 μL of AB-10B dye (100 μg mL^{-1}) was mixed with 600 μL MES buffer (50 mM, pH 6.8) containing 100 μL of Cu/H_3BTC MOF or laccase. At regular interval of every 5 min, sample was analysed for its concentration by measuring absorbance at 620 nm with UV-visible spectrophotometer to study the degradation efficacy. In each case, in order to get sequence of percent degradation, the obtained value of absorbance with regards to time was graphed. The subsequent equation was used to determine the degradation efficiency of AB-10B.[43]

$$\text{Degradation efficacy } \% = \frac{C_o - C_t}{C_o} \times 100$$

where C_o is the initial absorbance of dye and C_t is the dye solution absorbance at any given time.

2.5. Catalytic stability of Cu/H_3BTC MOF on AB-10B degradation

For cost-effective degradation of AB-10B by Cu/H_3BTC MOF, influence of various experimental parameters needs to be investigated. 100 μL of Cu/H_3BTC MOF was added to dye solution (300 μL, 100 μg mL^{-1}) and incubated in different pH (3.0–9.0) range of MES buffer (30 mM, 600 μL). The effect of thermal stability at different temperatures (30–90 °C) was measured by incubating AB-10B dye (300 μL, 100 μg mL^{-1}) with MES buffer (30 mM, 600 μL) containing 100 μL of Cu/H_3BTC MOF. The role of ionic strength was studied by contacting AB-10B dye solution (300 μL, 100 μg mL^{-1}) with Cu/H_3BTC MOF in diverse range of NaCl (500, 400, 300, 200, 100 and 0 mM). In evaluation of each parameter, freshly prepared samples were used in triplicates and determined the standard deviation by error bars. To evaluate long-term storage stability, Cu/H_3BTC MOF was kept at room temperature and residual activity at 620 nm was measured every day. For all these assays, same concentration of free laccase was assessed with the same procedure for comparative study and error bars were

determined from standard deviation of triplicate measurements. The multiple use of catalyst has crucial importance in order to abate expenses. For this purpose, reusability was calculated by measuring the activity change of Cu/H_3BTC MOF for approximately ten repeated steps using AB-10B dye (300 μL, 100 μg mL^{-1}). Hence after each step, the applied Cu/H_3BTC MOF was restored from the dye reaction mixture, washed with MES buffer (50 mM, pH 6.8) and was further introduced again in a fresh reaction mixture to measure the residual enzyme activity.

2.6. Laccase-like mimic activity of Cu/H_3BTC MOF

Chromogenic reaction of phenolic compounds with 4-AP was carried out to measure the catalytic activity of Cu/H_3BTC MOF and laccase. In brief, solution of 2,4-DP (100 μL, 1 mg mL^{-1}) and 4-AP (100 μL, 1 mg mL^{-1}) were added with MES buffer (700 μL, 30 mM, pH 6.8). Then aqueous suspension of Cu/H_3BTC MOF or laccase (100 μL, 1 mg mL^{-1}) was added. After 1 h of reaction at room temperature, centrifuged the reaction mixture (10 000 rpm, 2 min) and absorbance of the supernatant was measured at 510 nm *via* UV-visible spectrometer. To assess the catalytic mimic activity of Cu/H_3BTC MOF and laccase for various substrates, solutions of organic compounds like 2,4-DP, phenol, *p*-nitrophenol, naphthol, and catechol (100 μL, 1 mg mL^{-1}) were evaluated following the above-mentioned procedure.

2.7. Evaluation of catalytic stability of Cu/H_3BTC MOF

The pH of solution is a significant feature that can remarkably impact catalytic reactions. Thus, the consequence of pH on the stability of Cu/H_3BTC MOF was investigated at different pH range. The effect of pH on Cu/H_3BTC MOF was measured in MES buffer (30 mM) with different pH range from 3.0 to 9.0. The thermal constancy in diverse temperature range of 30 to 90 °C was determined by incubating Cu/H_3BTC MOF in MES buffer (30 mM, pH 6.8). In order to test the ionic strength, residual activity of Cu/H_3BTC MOF was assayed after being incubated in various NaCl concentrations (500, 400, 300, 200, 100 and 0 mM). Throughout these studies, the reaction was allowed for 1 h prior the supernatant absorptivity at 510 nm was monitored. All the samples were studied in triplicates and aligned the error bars by standard deviation. For comparison, same concentration of free laccase was assayed in the same way.

2.8. Catalytic oxidation of epinephrine by Cu/H_3BTC MOF and laccase

Samples of epinephrine (50 μL, 100 μg mL^{-1}) dissolved in hydrochloric acid (12 mM) was added with aqueous solution of Cu/H_3BTC MOF or laccase (1 mg mL^{-1}, 100 μL) and MES buffer (850 μL, 50 mM, pH 6.8) and observed their oxidation at wavelength 485 nm. In order to study the limit of detection, various concentrations of epinephrine were added with 0.1 mg mL^{-1} of Cu/H_3BTC MOF or laccase respectively in MES buffer and evaluated with $3\sigma/b$, whereas σ is the standard errors of blank signals and b is regression line of slope.

3. Results and discussion

The multi dentate benzene-1,3,5-tricarboxylate (H_3BTC) are excellent ligand which has great capability to coordinate with metal ions because of partial or complete deprotonation of the multi-carboxylate groups of H_3BTC ligand.[44,45] An arrangement of H_3BTC reacting with Cu^{2+} has been shown in Fig. 1, where H_3BTC contribute to coordinate with copper metal in order to form a novel network structure.[46]

3.1. Structural characterization of Cu/H_3BTC MOF

The XRD diffraction as shown in Fig. 2A were recorded to determine the phrase purity and crystallinity of Cu/H_3BTC MOF. The XRD pattern of Cu/H_3BTC MOF in which the characteristic peaks appeared at $2\theta = 9.5°$, 11.6°, 14.1°, 19.0°, 21.0°, 23.1°, 25.3°, 30.1°, 39.3° and 43.8° correspond to the (220), (222), (420), (440), (442), (551), (731), (751), (882), (231) and are in good agreement with their corresponding reported patterns in previous literature.[47–49] In the XRD patterns, no noticeable peak associated to impurity was detected.

The FTIR spectrum of Cu/H_3BTC MOF in the wavelength range of 500–4000 cm^{-1} was achieved to further figure out the binding arrangement of Cu with H_3BTC (Fig. 2B). The presence of a wide-ranging band at 2700 to 3500 cm^{-1} specifies the occurrence of –OH groups in Cu/H_3BTC structure.[50] The Cu/H_3BTC MOF show strong stretching vibration of the carboxylate anions at around 1643.86 cm^{-1}, verifying the reaction of –COOH groups in H_3BTC with copper ions.[49] Moreover, the presence of peaks at 1710 cm^{-1}, 1180 cm^{-1} and 1240 cm^{-1} are assigned to the vibrations of C=O, C–O and O–H groups.[51] Furthermore, the band appeared at 719 cm^{-1} might be due to the stretching mode of Cu–O.[52]

The structural order and morphology of Cu/H_3BTC MOF was examined by SEM and EDX. The as synthesized Cu/H_3BTC MOF exhibits a clear rod like structure of different sizes. These structures have regular and smooth shape having aspect ratio of approximately 80–100 nm (Fig. 3A). Furthermore, EDX was achieved to categorize the elemental composition of the prepared Cu/H_3BTC MOF, which exhibited the influence of C, O and Cu. The percent weight as indicated in the EDX was 35.78, 30.08 and 34.15 for C, O and Cu respectively (Fig. 3B).

Nitrogen adsorption and desorption isotherm was performed to determine the surface area plus distribution of pore

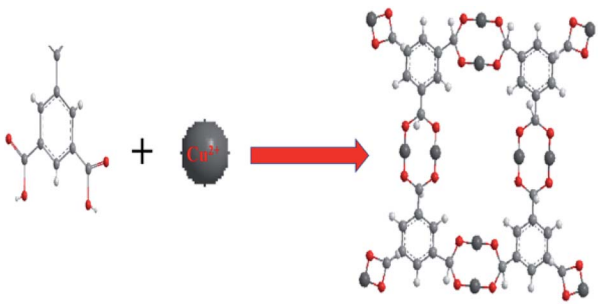

Fig. 1 Structure of Cu^{2+} reacting with H_3BTC to form Cu/H_3BTC MOF. Colour code: Cu (dark grey); O (red); C (light grey); H (white).

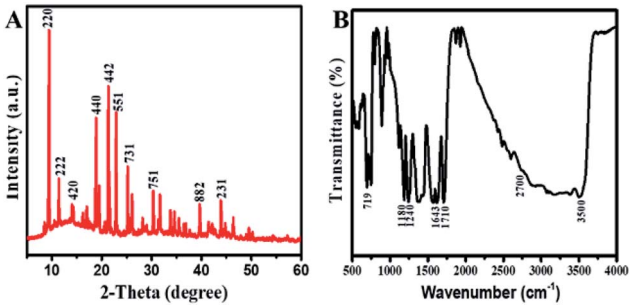

Fig. 2 (A) XRD patterns of freeze-dried Cu/H_3BTC MOF. (B) FTIR spectrum of Cu/H_3BTC MOF.

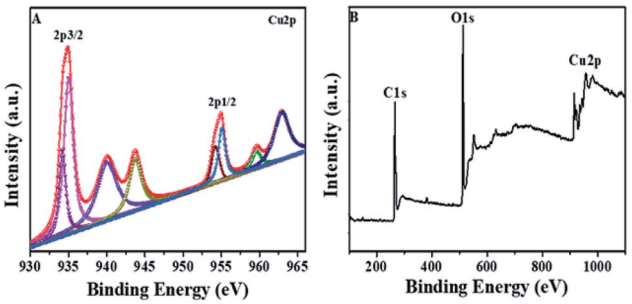

Fig. 4 (A) XPS spectrum of Cu 2p. (B) XPS fully scanned spectrum of Cu/H_3BTC MOF.

size and obtained the results using BJH (Barrett Joyner Halenda) model (Fig. 3C and D). The specific surface area is 9.60 $m^2\ g^{-1}$, which is higher than the reported value.[26] Pore size distribution was examined for the porosity which is 0.21 nm, hence the prepared CuH_3BTC MOF may be deliberated a micro capillary type material (<1 nm) which might be due to the lower reaction temperature that correspond to an increase in surface area and a decrease in particle size.[53]

XPS was done to study the oxidation number of Cu in Cu/H_3BTC MOF. The Cu/H_3BTC revealed a scale with a core region (Cu $2p_{2/3}$ and Cu $2p_{1/2}$) along with satellite peaks. In the XPS spectrum, the peaks at 934.9 and 955.01 eV (Fig. 4A) are attributed to the Cu $2p_{3/2}$ and Cu $2p_{1/2}$ electrons of Cu^{2+} respectively.[54] Peaks having lower binding energy at 934.2 and 954.3 eV indicate the occurrence of Cu^0 or Cu^+.[55] Moreover, the full-scan spectrum also illustrates the existence of Cu, O and C (Fig. 4B). In addition, the Auger Cu LMM spectrum showed the detailed oxidation state of copper in Cu/H_3BTC MOF and supported the existence of Cu^+ and Cu^{2+} at 572.9 eV, 568.2 eV respectively (Fig. S1†). Hence, in the formation reaction of Cu/H_3BTC MOF a portion of Cu^{2+} is reduced to Cu^+ which could elucidate the greater activity of Cu/H_3BTC MOF. Finally, in order to address the stability of Cu/H_3BTC MOF, zeta-potential was performed. The value of zeta-potential is in negative, approximately near to zero (Fig. S2†) which might elucidate their long-term stability and the formation of dispersed stable nanoparticles.[56]

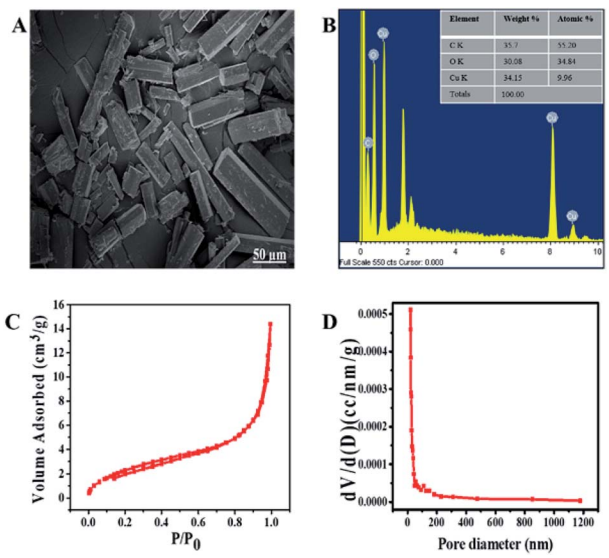

Fig. 3 (A) SEM (B) EDX spectrum (inset) percent composition. (C) Nitrogen adsorption/desorption isotherm of Cu/H_3BTC MOF to measure the specific surface area. (D) Distribution of pore size of Cu/H_3BTC MOF.

3.2. Laccase like activity of Cu/H_3BTC MOF

Laccase activity assay process involving the substrate 2,4-DP along with 4-AP was used to evaluate the probability of such a ligand incorporated copper as laccase mimic. 2,4-DP is the actual substrate which yield a red adduct by reacting its laccase catalysed oxidation product with 4-AP (Fig. S3A†). These observations showed that Cu/H_3BTC MOF exhibit laccase-like catalytic activity. A control experiment was also done *via* reacting substrates with free Cu^{2+} in water as the free Cu^{2+} could catalyse such reaction as well. As a result, light-pink colour was obtained as compared to Cu/H_3BTC MOF (Fig. S3B†). This specifies that single Cu^{2+} has a reasonable activity.

To distinguish the basic evidence intended for catalysis, different MOFs were prepared by intermixing of Cu^{2+} with H_3BTC, GMP, AMP, CMP and guanosine, which yield a light blue colour in each case (Fig. 5A, upper tubes). All these samples were active as specified by appearance of reddish colour of resultant product after mixing with 2,4-DP and 4-AP (Fig. 5A, lower tubes). From the results in Fig. 5B it was observed that Cu/H_3BTC MOF has better activity. Therefore, we follow Cu/H_3BTC MOF for further study.

Afterward studying the ligand requirement, the incorporation of few metal ions including transition metals to make mixed metal composite was studied. Although most of it precipitated with H_3BTC ligand (Fig. 5C, above tubes) but their activity was very low, almost show no activity (Fig. 5C, below tubes). Accordingly, the activity of Cu is significant and same as natural laccases.

Overall, Cu/H_3BTC MOF as laccase mimic is simple to prepare and optimization of the catalyst concentration (Cu/H_3BTC) is most important for effective activity. In order to identify the optimized catalyst concentration, Cu/H_3BTC MOF

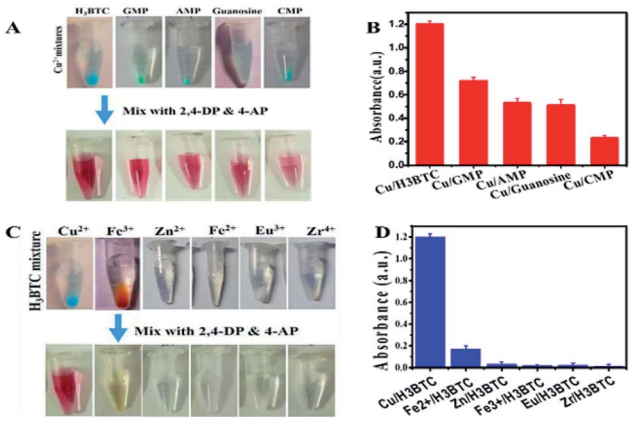

Fig. 5 Photos of MOFs prepared (A) by mixing Cu^{2+} with different nucleotides, guanosine and (C) by mixing H_3BTC with several metal ions. (B and D) Laccase-like activity by assessing 2,4-DP and 4-AP (0.1 mg mL^{-1}) with different nucleotides/metal (0.1 mg mL^{-1}) in MES buffer pH 6.8.

and laccase were thoroughly compared at various concentrations. It is interesting to note that greater activity of both laccase and Cu/H_3BTC MOF was detected with higher catalyst concentration as shown in Fig. S6A† which can be justified that the number of active sites increased with increase of catalyst concentration.[57] At concentration less than 0.1 mg mL^{-1} Cu/H_3BTC MOF showed higher activity compared with laccase. Hence, following activities were then implemented at such concentration.

3.3. Degradation of AB-10B at different time intervals

In order to verify the degradation of AB-10B dye molecule, some spectral analysis at optimum conditions was also performed. Degradation of AB-10B by Cu/H_3BTC MOF was studied by evaluating UV-visible spectral changes in the range of 200–700 nm at different time intervals. The variation in the absorption spectrum of AB-10B dye at different intervals of time are presented in Fig. 6A. It is noticeable from resulting spectrum that before treating the sample with Cu/H_3BTC MOF, a broad band was observed in UV-visible region at 620 nm followed by two sharp peaks in ultraviolet regions at 226 nm and 318 nm. The peak at 620 nm was accredited to the n → π* transition of –N=N– group, the main conjugates of AB-10B, while two peaks at ultraviolet regions (226 nm and 318 nm) was due to absorption of π → π* transition of benzene ring and naphthalene ring.[50] It was observed clearly that after addition of Cu/H_3BTC MOF, the absorption peak declined very quickly with the passage of time and approximately vanished completely within 60 min. These spectral changes indicated the degradation of AB-10B dye in the presence of Cu/H_3BTC MOF. In addition to the decreased of absorption peak, we observed blue shift (hypsochromic shift) simultaneously in maximum absorption wavelength of AB-10B with increasing irradiation time. This blue shift indicates the presence of different intermediates produced and could also be attributed to reduced absorbance value of the decomposed products.[58–60] Moreover, the diminution of absorption peaks in visible and UV regions clearly demonstrated that Cu/H_3BTC MOF was also effective for the cleavage and degradation of the aromatic structures of dye molecule. In comparison, degradation activity of laccase was also evaluated as shown in Fig. 6B. From the result, it was inferred that the laccase degradation activity was slightly increase with the passage of time but resulted in a much slower, nearly negligible and insignificant loss of dye whereas this difference was higher and more noticeable at same concentration of Cu/H_3BTC MOF. Hence, it suggested that complete and rapid degradation of AB-10B dye has been completed in presence of Cu/H_3BTC MOF and might be applicable for the practical dye containing wastewater to some extent.

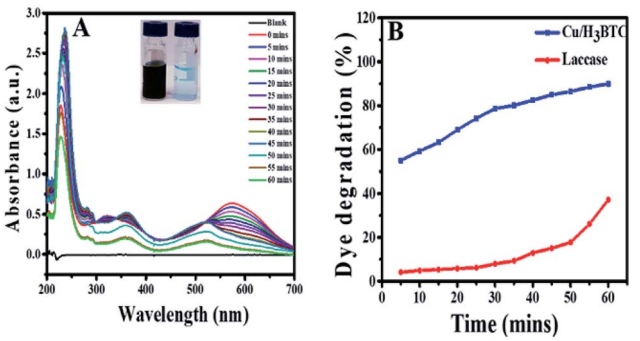

Fig. 6 (A) AB-10B dye degradation with Cu/H_3BTC MOF and UV-vis spectra were recorded every five minutes (till 60 min), (inset) before and after degradation. (B) percent degradation of AB-10B catalysed by Cu/H_3BTC MOF or laccase as function of time.

3.4. Degradation stability and recyclability of Cu/H_3BTC MOF

The effect of experimental parameters such as pH, temperature, ionic strength, storage time and the recyclability of Cu/H_3BTC MOF on the decolorization and degradation AB-10B dye was investigated in order to optimize the possible analytical method. Dye degradation and enzymatic reactions are well known to be pH dependent and an essential factor in wastewater treatment.[61,62] Moreover, pH of solution is a main factor which influences dye degradation as pH affects the surface charge properties of the catalyst.[63] Hence, to optimize reaction pH for AB-10B dye degradation, the considered range of pH was 3.0 to 9.0 as illustrated in Fig. 7A. The results specified that the degradation of AB-10B dye was highly affected in the course of solution pH. At low pH, degradation efficiency was slowed while there is a prominent improvement in the degradation efficiency (90%) along with increasing of pH (up to 6.8) value. This behaviour can be explained on the basis of stability and surface charge density of the Cu/H_3BTC MOF as shown by measured zeta potential in Fig. S2.† Degradation of dye enhanced at pH 6.8 because at this pH Cu/H_3BTC MOF has negative charged density due to deprotonated COOH groups and dye exhibits positive charge. Hence, when the dye adsorbed on Cu/H_3BTC MOF, electronic induction takes place towards the cationic NH_2 and electron withdrawing NO_2 groups of dye. This induction

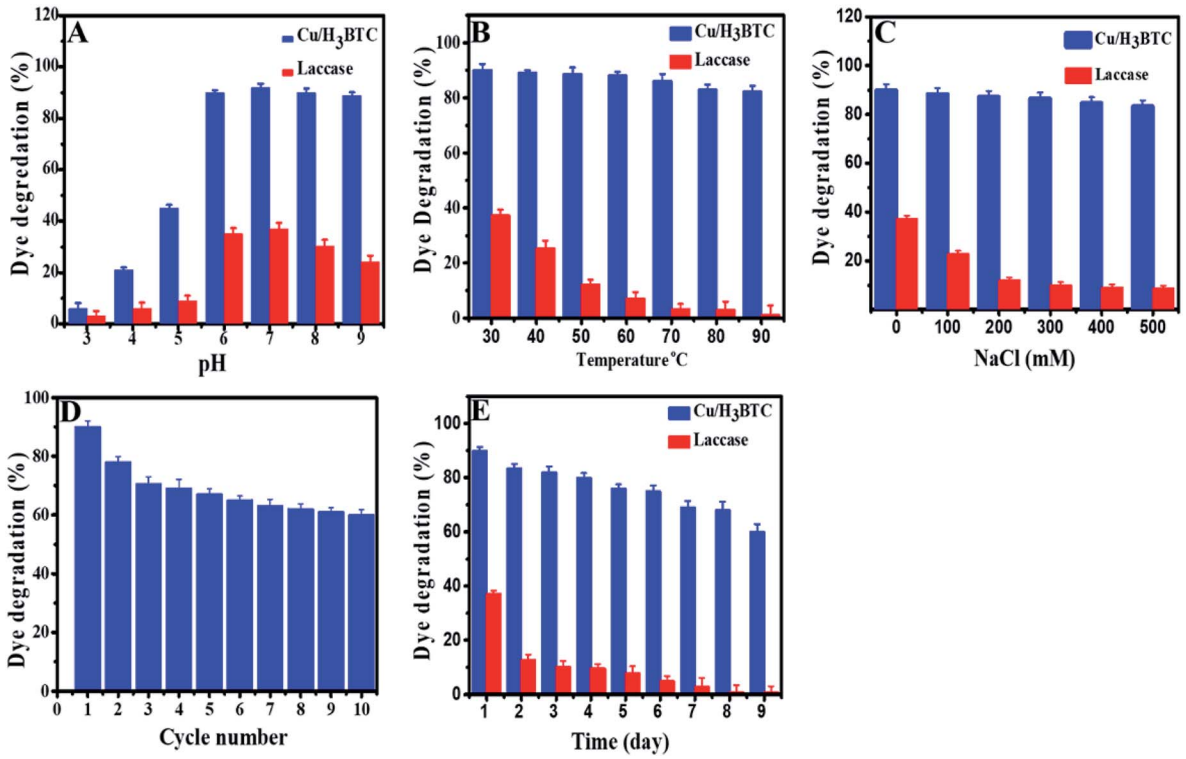

Fig. 7 Efficiency of Cu/H_3BTC MOF and laccase on percent degradation at different (A) pH (B) temperature (C) NaCl concentration (D) reusability of Cu/H_3BTC MOF (E) storage stability of Cu/H_3BTC MOF and laccase.

weakens the azo bond of dye, resulted in the degradation of dye. As the pH of the system further increases, degradation of dye decreases. The decreased degradation efficiency at high pH is due to the appearance of repulsive forces between the highly negatively charged catalyst and the anionic dye molecules, causing the decrease in adsorption of AB-10B and consequently reducing the percent degradation.[64,65] Therefore, a pH of 6.8 is more favourable and was applied in following experimental work. However, free laccase has very low ability to degrade AB-10B dye and further increasing of pH has no effect on the degradation efficiency. This can be explained on the basis that in degradation experiments, the chemical structure of applicable dyes possesses a critical role as generally azo dyes are found to be resistant to laccase-based degradation. One the other hand anthraquinone dyes are appropriate substrate for laccases.[66]

The dye degradation was also monitored as a function of temperature. Fig. 7B, shows the influence of temperature on percent degradation of AB-10B dye by laccase and Cu/H_3BTC MOF. The results illustrated that the degradation process by Cu/H_3BTC MOF is critically dependent on temperature and increased dramatically with an increase in temperature. Interestingly, Cu/H_3BTC MOF was found to be active and retain its activity even at 90 °C. However, laccase appears to work well at 30 °C and the degradation activity was significantly suppressed with further increase of temperature, specifying the decline of chemical stability of enzyme beyond room temperature. This may be due to deactivation of the enzymes responsible for degradation.[67]

Laccase is frequently use as a catalyst in water treatment.[68] Therefore, the impact of various concentration of ionic strength on degradation of AB-10B by laccase and Cu/H_3BTC MOF was also studied (Fig. 7C). The results described that the efficacy of dye degradation by Cu/H_3BTC MOF was not considerably influenced with ever-increasing of NaCl concentration and showed higher degradation percent. However, laccase had insufficient capacity to degrade dye molecules and upon increasing of NaCl concentration, laccase activity decreases drastically because high ionic strength affected the enzyme spatial structure and charge distribution, causing deactivation of laccase.[69]

From industrial point of view, it is very important to know reusability of Cu/H_3BTC MOF in order to reduce costs. Stability of the Cu/H_3BTC MOF, as a critical property for large-scale operations was evaluated by running several recycling degradations processes. The reusability of the Cu/H_3BTC MOF was studied by mixing of AB-10B dye with Cu/H_3BTC MOF in MES buffer and kept at 25 °C for 1 h. After 1 h, the Cu/H_3BTC MOF was collected by centrifugation, washed with deionized water and reused for the next reaction cycle. Reducing profile of percent degradation during ten cycles has been shown in Fig. 7D. The results demonstrated that our designed Cu/H_3BTC MOF has a strong influence on degradation activity and retain 60% of its initial activity after ten cycles. The results also

showed that Cu/H_3BTC MOF can be restored and can be reused for at least ten successive cycles.

Furthermore, storage stability of Cu/H_3BTC MOF and laccase was elucidated by storing these at −4 °C for 9 days. The results in Fig. 7E indicated that dye degradation ability of Cu/H_3BTC MOF remained active even for a period of 9 days. Conversely, laccase activity under the same storage conditions was completely deactivated within 9th day and degradation process stopped, signifying good storage stability of Cu/H_3BTC MOF as compared to laccase.

3.5. Catalytic detection of phenolic pollutants by Cu/H_3BTC MOF

Laccase is a member of the MCOs (multicopper oxidases) capable of oxidizing a wide range of substrates as a result of a radical-catalysed reaction mechanism.[70] The substrate diversity of Cu/H_3BTC MOF can be assessed by mixing it with some phenolic compounds and 4-AP (chromogenic agent). The chemical structure of these phenolic compounds are given in Fig. 8A. It was found that Cu/H_3BTC MOF has the capability to oxidize each of them with enhanced catalytic efficacy as compared to same dosage of laccase in individual case, signifying the favourable substrate universality of Cu/H_3BTC MOF (Fig. 8B). Similar studies was also performed by other scientists and it was found that Cu/H_3BTC MOF is more robust to oxidize diverse range of substrates at higher catalytic rate.[71,72] These phenols are significant industrial chemicals and might induce environmental issues. Be able to efficiently oxidize them is strongly recommended.

3.6. Detection of epinephrine based on Cu/H_3BTC MOF

Further environmental application of Cu/H_3BTC MOF was demonstrated by measuring epinephrine. Epinephrine produced by adrenal medulla, reduces the allergens creating reaction, minimize breathing difficulties and also help to treat organ, heart disease and bronchial asthma. Hence, for diagnosis and pharmaceutical analysis its quantitative study is necessary. Laccase and Cu/H_3BTC MOF was individually treated with epinephrine and as a result coloured product was produced, which indicated that Cu/H_3BTC MOF is even capable to oxidize epinephrine (Fig. 9A). Various concentrations of epinephrine (5 to 50 μg mL^{-1}) were mixed with Cu/H_3BTC MOF or laccase and measured the oxidized product at 485 nm. As shown in Fig. 9B, the absorbance of the oxidized product at 485 nm enhanced as a function of epinephrine concentration catalysed by same quantity of Cu/H_3BTC MOF or laccase. The results also showed that Cu/H_3BTC MOF is more susceptible than laccase due to greater catalytic activity of Cu/H_3BTC MOF and might be used as a procedure for epinephrine detection. Furthermore, Fig. 9D indicated that in the initial twenty minutes, the reaction kinetics with the Cu/H_3BTC MOF is quicker as compared to laccase. Moreover, the reaction kinetic parameters of the Cu/H_3BTC MOF and laccase were elucidated by the Michaelis–Menten model (Fig. S5†). The K_m of laccase is lesser than that of Cu/H_3BTC MOF, representing higher affinity of substrate due to its flexible structure compared with the rigid structure of the Cu/H_3BTC MOF. However, V_{max} of Cu/H_3BTC MOF is much greater than that of laccase, which is possibly referable to its multinuclear arrangement of Cu^{2+} and is comparable to laccase and can aid as a better functional mimic.

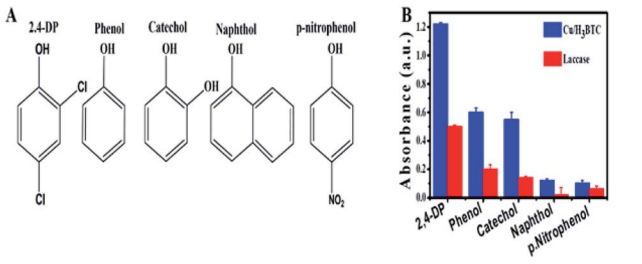

Fig. 8 (A) The chemical structures of different tested phenols. (B) Catalytic efficacy of laccase and Cu/H_3BTC MOF to oxidize substrates.

3.7. Catalytic stability of Cu/H_3BTC MOF

Studies based on stability are significant parameter to be considered for practical applications. To test the stability feature in various harsh conditions, laccase and Cu/H_3BTC MOF were compared in several experimental conditions (Fig. S6B–D†). First of all, they were exposed to MES buffers of different pH range from 3.0 to 9.0 at room temp for 1 h. As shown in Fig. S6B,† laccase lost almost 70% of its catalytic activity after incubation in a pH 3.0 and 9.0 buffer while the laccase mimic Cu/H_3BTC MOF retain its stability up to pH 9.0 with over 200% residual activity after incubation. Moreover, higher stability of Cu/H_3BTC MOF at optimum pH 6.8 specifies the appreciably improved stability of Cu/H_3BTC MOF as compared to laccase. This difference in activity might be electrostatic repulsion at high pH, which led to failure to decompose the substrate.[1]

The thermal stability of laccase and Cu/H_3BTC MOF with regard to relative activities are compared as illustrated in Fig. S6C.† It can be seen that the relative activity of laccase was much lower than Cu/H_3BTC MOF and gradually declined at each temperature. Also, laccase almost lost its catalytic activity beyond 60 °C, showing that laccase was extremely sensitive and easily deactivated after treatment at a relatively high temperature. However, the function of Cu/H_3BTC MOF was not affected by thermic treatment and exhibited high thermal tolerance from 30 °C to 80 °C. When incubated at 90 °C for 60 min, the catalytic activity of Cu/H_3BTC MOF decreases, significantly the regression of thermal stability of Cu/H_3BTC MOF beyond 90 °C.

The influence of ionic ability on catalytic efficiency was furthermore examined (Fig. S6D†). The results showed that activity of laccase suppressed at high NaCl concentration which might be due to charge distribution and degeneration of enzyme active centre. While for Cu/H_3BTC MOF, the rate of reaction continuously increases as the ionic strength increases and it is very curious that even with 500 mM NaCl its catalytic performance increased by ~300%.

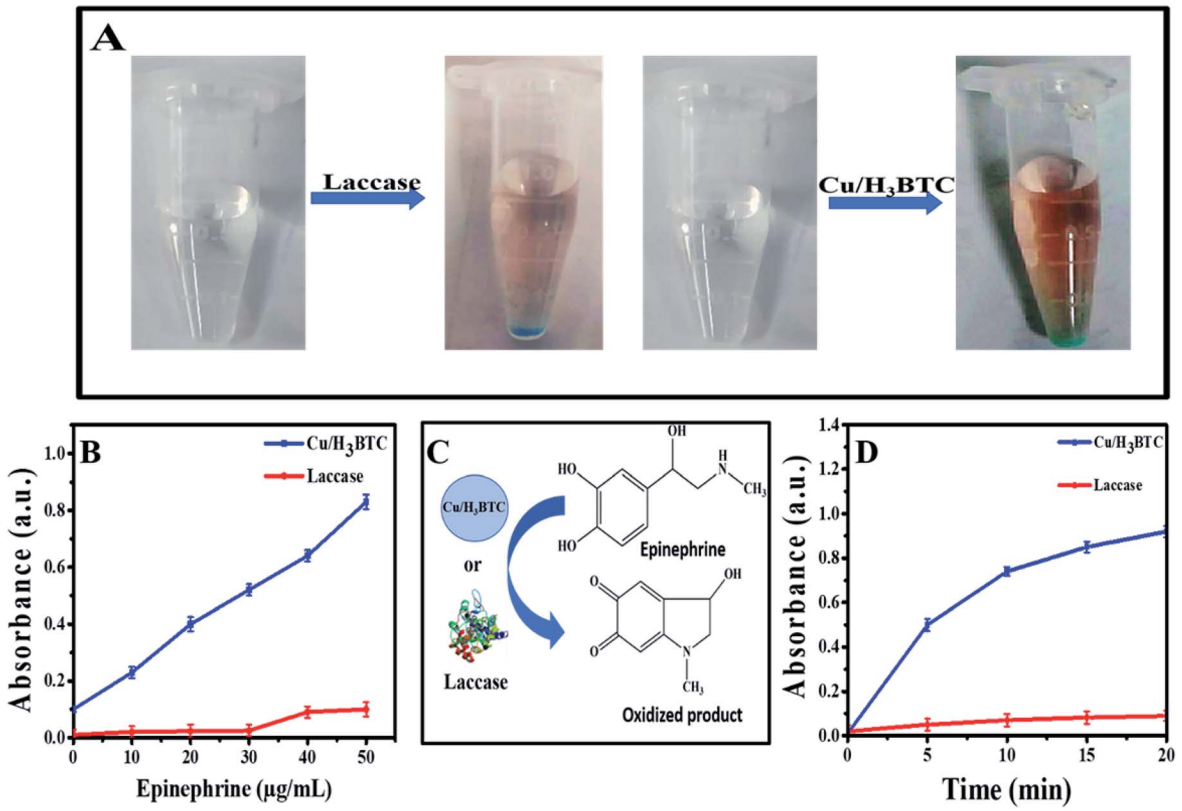

Fig. 9 (A) Sketch and photographs of oxidizing epinephrine. (B) Kinetics oxidization of epinephrine (50 μg mL^{-1}) with 0.1 mg mL^{-1} of laccase or Cu/H_3BTC MOF. (C) Scheme of oxidizing epinephrine. (D) Linear correlations among concentration of epinephrine and absorbance in presence of laccase and Cu/H_3BTC MOF.

4. Conclusion

To conclude, mimic laccase Cu/H_3BTC MOF with laccase like activities was synthesized by a simple novel strategy using H_3BTC coordinated Cu^{2+}. Laccase mimic activity of Cu/H_3BTC MOF was assessed using a laccase substrate 2,4-DP. We used the as synthesized Cu/H_3BTC MOF as a mimic enzyme for effective degradation of AB-10B dye and found that catalytic performance of Cu/H_3BTC MOF on AB-10B dye was greater than natural enzyme with profound reusability and storage stability. The UV-vis spectral changes of AB-10B dye indicated that Cu/H_3BTC MOF is more convenient to destruct AB-10B dye. The prepared Cu/H_3BTC MOF showed excellent stability under different conditions as compared with natural laccase. Just as laccase, Cu/H_3BTC MOF converts a wide range of substrates with higher catalytic rate. Present study proves that Cu/H_3BTC MOF have significant ability in azo dye degradation and enzyme catalysis. On the other hand, excellent catalytic activity, high stability, recyclability and substrate ubiquity proves its promising utilization in catalysis and rapid detection. Therefore, this material is proposed as an appropriate method for water treatment contaminated with AB-10B and will probably seek significant demands to interchange the function of laccase in various fields.

Conflicts of interest

The authors declare no conflict of interest.

Acknowledgements

The authors acknowledged financial support from the Chinese scholarship Council (Grant No 2016GXYS68), National Natural Science Foundation of China (21878014), the Beijing Natural Sciences Foundation (2162030), and Beijing Municipal Education Commission Joint Funding Project (KZ201710020014), the Double First-rate Program (ylkxj03) and the 111 Project (B13005).

References

1 J. H. Sun, S. P. Sun, G. L. Wang and L. P. Qiao, *Dyes Pigm.*, 2007, **74**, 647–652.
2 H. Park and W. Choi, *J. Photochem. Photobiol. A Chem.*, 2003, **159**, 241–247.
3 Y. Huang, Z. Wang, Q. Liu, X. Wang, Z. Yuan and J. Liu, *Chemosphere*, 2017, **187**, 338–346.
4 E. Haque, J. W. Jun and S. H. Jhung, *J. Hazard. Mater.*, 2011, **185**, 507–511.
5 A. Córdoba, I. Magario and M. L. Ferreira, *Int. Biodeterior. Biodegrad.*, 2012, **73**, 60–72.
6 V. Karthik, K. Saravanan, P. Bharathi, V. Dharanya and C. Meiaraj, *J. Chem. Pharm. Sci.*, 2014, **7**, 301–307.
7 S. Akhtar, A. A. Khan and Q. Husain, *Chemosphere*, 2005, **60**, 291–301.

8 Q. Yang, M. Yang, K. Pritsch, A. Yediler, A. Hagn, M. Schloter and A. Kettrup, *Biotechnol. Lett.*, 2003, **25**, 709–713.
9 A. L. Hu, H. H. Deng, X. Q. Zheng, Y. Y. Wu, X. L. Lin, A. L. Liu, X. H. Xia, H. P. Peng, W. Chen and G. L. Hong, *Biosens. Bioelectron.*, 2017, **97**, 21–25.
10 A. Ahmed, A. Abagana, D. Cui and M. Zhao, *Biomed Res. Int.*, 2019, DOI: 10.1155/2019/7127869.
11 A. H. Memon, R. Ding, Q. Yuan, H. Liang and Y. Wei, *Biochem. Eng. J.*, 2018, **136**, 102–108.
12 X. Wang, Y. Hu and H. Wei, *Inorg. Chem. Front.*, 2016, **3**, 41–60.
13 W. He, X. Wu, J. Liu, X. Hu, K. Zhang, S. Hou, W. Zhou and S. Xie, *Chem. Mater.*, 2010, **22**, 2988–2994.
14 N. Puvvada, P. K. Panigrahi, D. Mandal and A. Pathak, *RSC Adv.*, 2012, **2**, 3270–3273.
15 J. Xie, X. Zhang, H. Wang, H. Zheng and Y. Huang, *Trends Anal. Chem.*, 2012, **39**, 114–129.
16 C. G. Kumar and P. Mongolla, *Environ. Sci. Eng. (Subseries Environ. Sci.)*, 2015, pp. 85–110.
17 D. M. Mate and M. Alcalde, *Biotechnol. Adv.*, 2015, **33**, 25–40.
18 C. Galli, C. Madzak, R. Vadalà, C. Jolivalt and P. Gentili, *ChemBioChem*, 2013, **14**, 2500–2505.
19 X. Wang, J. Liu, R. Qu, Z. Wang and Q. Huang, *Sci. Rep.*, 2017, **7**, 1–10.
20 S. Eyele-Mezui, P. Vialat, C. Higy, R. Bourzami, C. Leuvrey, N. Parizel, P. Turek, P. Rabu, G. Rogez and C. Mousty, *J. Phys. Chem. C*, 2015, **119**, 13335–13342.
21 C. Uhlmann, I. Swart and J. Repp, *Nano Lett.*, 2013, **13**, 777–780.
22 L. Zhou, D. Powell and K. M. Nicholas, *Inorg. Chem.*, 2007, **46**, 7789–7799.
23 Y. Tanaka, W. Hoshino, S. Shimizu, K. Youfu, N. Aratani, N. Maruyama, S. Fujita and A. Osuka, *J. Am. Chem. Soc.*, 2004, **126**, 3046–3047.
24 M. Verónica Rivas, L. P. Méndez De Leo, M. Hamer, R. Carballo and F. J. Williams, *Langmuir*, 2011, **27**, 10714–10721.
25 X. Ren, J. Liu, J. Ren, F. Tang and X. Meng, *Nanoscale*, 2015, **7**, 19641–19646.
26 H. Liang, F. Lin, Z. Zhang, B. Liu, S. Jiang, Q. Yuan and J. Liu, *ACS Appl. Mater. Interfaces*, 2017, **9**, 1352–1360.
27 I. Nath, J. Chakraborty and F. Verpoort, *Chem. Soc. Rev.*, 2016, **45**, 4127–4170.
28 M. J. Wiester, P. A. Ulmann and C. A. Mirkin, *Angew. Chem., Int. Ed.*, 2011, **50**, 114–137.
29 R. W. Larsen, L. Wojtas, J. Perman, R. L. Musselman, M. J. Zaworotko and C. M. Vetromile, *J. Am. Chem. Soc.*, 2011, **133**, 10356–10359.
30 J. Zheng, Y. Wu, K. Deng, M. He, L. He, J. Cao, X. Zhang, Y. Liu, S. Li and Z. Tang, *ACS Nano*, 2016, **10**, 8564–8570.
31 C. Li, K. Deng, Z. Tang and L. Jiang, *J. Am. Chem. Soc.*, 2010, **132**, 8202–8209.
32 S. Duan, J. Li, X. Liu, Y. Wang, S. Zeng, D. Shao and T. Hayat, *ACS Sustain. Chem. Eng.*, 2016, **4**, 3368–3378.
33 K. A. Cychosz, A. G. Wong-Foy and A. J. Matzger, *J. Am. Chem. Soc.*, 2008, **130**, 6938–6939.
34 L. Hamon, C. Serre, T. Devic, T. Loiseau, F. Millange, G. Férey and G. De Weireld, *J. Am. Chem. Soc.*, 2009, **131**, 8775–8777.
35 H. Yu, S. Zhang, M. R. Dunn and J. C. Chaput, *J. Am. Chem. Soc.*, 2013, **135**, 3583–3591.
36 P. Ballester, *Chem. Soc. Rev.*, 2010, **39**, 3810–3830.
37 K. Ruiz-Mirazo, C. Briones and A. de la Escosura, *Chem. Rev.*, 2014, **114**, 285–366.
38 Y. Liu and Z. Tang, *Chem.–Eur. J.*, 2012, **18**, 1030–1037.
39 P. Zhou, R. Shi, J.-f. Yao, C.-f. Sheng and H. Li, *Coord. Chem. Rev.*, 2015, **292**, 107–143.
40 J. An, S. J. Geib and N. L. Rosi, *J. Am. Chem. Soc.*, 2009, **131**, 8376–8377.
41 R. Nishiyabu, N. Hashimoto, T. Cho, K. Watanabe, T. Yasunaga, A. Endo, K. Kaneko, T. Niidome, M. Murata, C. Adachi, Y. Katayama, M. Hashizume and N. Kimizuka, *J. Am. Chem. Soc.*, 2009, **131**, 2151–2158.
42 H. A. Azab, Z. M. Anwar and R. G. Ahmed, *J. Chem. Eng. Data*, 2010, **55**, 459–475.
43 M. Iqbal, A. A. Thebo, A. H. Shah, A. Iqbal, K. H. Thebo, S. Phulpoto and M. A. Mohsin, *Inorg. Chem. Commun.*, 2017, **76**, 71–76.
44 X. Wang, M. Le, H. Lin, J. Luan, G. Liu and D. Liu, *Dalton Trans.*, 2015, **44**, 14008–14018.
45 J. C. Dai, X. T. Wu, Z. Y. Fu, C. P. Cui, S. M. Hu, W. X. Du, L. M. Wu, H. H. Zhang and R. Q. Sun, *Inorg. Chem.*, 2002, **41**, 1391–1396.
46 X. L. Wang, J. Li, H. Y. Lin, H. L. Hu, B. K. Chen and B. Mu, *Solid State Sci.*, 2009, **11**, 2118–2124.
47 F. Abbasloo, S. A. Khosravani, M. Ghaedi, K. Dashtian, E. Hosseini, L. Manzouri, S. S. Khorramrooz, A. Sharifi, R. Jannesar and F. Sadri, *Ultrason. Sonochem.*, 2018, **42**, 237–243.
48 R. Kaur, A. Kaur, A. Umar and W. A. Anderson, *Mater. Res. Bull.*, 2019, **109**, 124–133.
49 N. Tabatabaei, K. Dashtian, M. Ghaedi, M. M. Sabzehmeidani and E. Ameri, *New J. Chem.*, 2018, **42**, 9720–9734.
50 A. Goudarzi, A. D. Namghi and C. S. Ha, *RSC Adv.*, 2014, **4**, 59764–59771.
51 N. T. Phuong, C. Buess-Herman, N. T. Thom, P. T. Nam, T. D. Lam and D. T. M. Thanh, *Green Process. Synth.*, 2016, **5**, 537–547.
52 Y. Li and R. T. Yang, *AIChE J.*, 2015, **61**, 857–866.
53 K. J. Kim, Y. J. Li, P. B. Kreider, C. H. Chang, N. Wannenmacher, P. K. Thallapally and H. G. Ahn, *Chem. Commun.*, 2013, **49**, 11518–11520.
54 A. Jawad, Y. Li, L. Guo, A. Khan, Z. Chen, J. Wang, J. Yang, W. Liu and G. Yin, *RSC Adv.*, 2016, **6**, 72643–72653.
55 T. Ghodselahi, M. A. Vesaghi, A. Shafiekhani, A. Baghizadeh and M. Lameii, *Appl. Surf. Sci.*, 2008, **255**, 2730–2734.
56 A. Lopez and J. Liu, *J. Phys. Chem. C*, 2013, **117**, 3653–3661.
57 K. Govindan, H. T. Chandran and M. Raja, *J. Photochem. Photobiol. A Chem.*, 2017, **341**, 146–156.
58 G. Cinelli, F. Cuomo, L. Ambrosone, M. Colella, A. Ceglie, F. Venditti and F. Lopez, *J. Water Process Eng.*, 2017, **20**, 71–77.

59 I. A. Mir, I. Singh, B. Birajdar and K. Rawat, *Water Conservation Science & Engineering*, 2017, **2**, 43–50.
60 W. Ahmad, S. Shams, A. Ahmad, Y. Wei, Q. Yuan and A. Ullah, *Appl. Nanosci.*, 2019, DOI: 10.1007/s13204-019-01213-z.
61 S. S. Mirzadeh, S. M. Khezri, S. Rezaei, H. Forootanfar, A. H. Mahvi and M. A. Faramarzi, *J. Environ. Health Sci. Eng.*, 2014, **12**, 1–9.
62 K. Ahmad, A. H. Shah, B. Adhikari, U. A. Rana, S. N. Uddin, C. Vijayaratnam, N. Muhammad, S. Shujah, A. Rauf, H. Hussain, A. Badshah, R. Qureshi, H. B. Kraatz and A. Shah, *RSC Adv.*, 2014, **4**, 31657–31665.
63 K. Govindan, M. Raja, S. U. Maheshwari and M. Noel, *Environ. Sci.: Water Res. Technol.*, 2015, **1**, 108–119.
64 M. Tanzifi, M. T. Yaraki, A. D. Kiadehi, S. H. Hosseini, M. Olazar, A. K. Bhati, S. Agarwal, V. K. Gupta and A. Kazemi, *J. Colloid Interface Sci.*, 2018, **510**, 246–261.
65 Y. Wang, G. Xia, C. Wu, J. Sun, R. Song and W. Huang, *Carbohydr. Polym.*, 2015, **115**, 686–693.
66 U. Kalsoom, S. S. Ashraf, M. A. Meetani, M. A. Rauf and H. N. Bhatti, *Chem. Cent. J.*, 2013, **7**, 1.
67 E. G. Solozhenko, N. M. Soboleva and V. V. Goncharuk, *Water Res.*, 1995, **29**, 2206–2210.
68 P. Giardina, V. Faraco, C. Pezzella, A. Piscitelli, S. Vanhulle and G. Sannia, *Cell. Mol. Life Sci.*, 2010, **67**, 369–385.
69 F. Xu, *Biochemistry*, 1996, **35**, 7608–7614.
70 O. Farver, S. Wherland, O. Koroleva, D. S. Loginov and I. Pecht, *FEBS J.*, 2011, **278**, 3463–3471.
71 J. Wang, R. Huang, W. Qi, R. Su, B. P. Binks and Z. He, *Appl. Catal., B*, 2019, **254**, 452–462.
72 S. Pang, Y. Wu, X. Zhang, B. Li, J. Ouyang and M. Ding, *Process Biochem.*, 2016, **51**, 229–239.

